Available online www.ejaet.com

European Journal of Advances in Engineering and Technology, 2018, 5(7): 481-487

Research Article ISSN: 2394 - 658X

Study of a rectangular superconducting patch antenna and the influence of uniaxial electric anisotropy and temperature on resonant frequency and bandwidth

Abdelouahab Bouraiou[1], Tarek Fortaki[1] and Sihem Benkouda[2]

[1]*Electronics Department, University of Batna, 05000 Batna, Algeria*
[2]*Electronics Department, University of Frères Mentouri - Constantine 1, 25000 Constantine, Algeria*
E-Mail: bouraiou28@yahoo.fr

ABSTRACT
In order to see the parameters that can improve the performance of the antenna, and especially the bandwidth, we will study the resonance characteristics of an antenna with a superconducting rectangular microband patch at high critical temperature. The patch is printed on a uniaxial anisotropic substrate using the spectral approach together with the boundary condition of the complex resistivity on the superconducting patch. The models proposed was studied for the surface impedance of the antenna for a thin patch, and knowing that in previous studies [2], [3] studied substrate is a non-magnetic anisotropic substrate, for this work, we considered a substrate with electrical anisotropy as well as a magnetic anisotropy. Both the permittivity and permeability tensors are included in the mathematical formulation of the problem. We calculated the influence of the variation of the electric permittivity on the frequency and especially on the bandwidth with temperatures near and far from Tc.

Key words: Superconducting, uniaxial anisotropy, permittivity tensor, permeability tensor

1. INTRODUCTION

The great areas of human civilization bear the names of the most important material of the time, for example, in the Stone Age people understood that the stone can serve them in everyday life, after, later, to the Iron Age and the Bronze Age, people have been able to transform the material, and this is since the human being has not stopped discovering more and more other materials according to the needs of each period. In the 19th century, steel was the material most used for the industrial revolution.

In the 20th century, it can be said that it is the century of the immense revolution of computing and telecommunications; and without a doubt, the most used material in all electronic instruments and devices and that helped realize them and that directly contributed to this huge leap of human civilization is silicon. For the 21st century, researchers are still looking to improve existing materials, as well as trying to make other materials that can help avoid the disadvantages of conventional materials. Several researches in the world have been made on new materials, and among these new materials that can be the materials of the century we find the superconductors.

The class of cuprates (or superconductors at high critical temperature (Tc)), discovered in 1986, has superconducting properties at higher temperatures than conventional superconductors. The surface resistance of the relatively low critical temperature superconducting film facilitates the development microwave devices with better performance than conventional devices. Studies on this type of superconducting antenna at high critical temperature have shown that they have a high gain compared to conventional antennas, but with a very narrow bandwidth, which limits their applications [1-2]. In addition to the remarkable interest in high critical temperature superconducting materials, there is also a growing interest in the study of microwave circuits on anisotropic substrates, especially uniaxial anisotropy [2-3].

The interest in the study of anisotropic substrates comes from two main arguments: the first is that substrates in practice exhibit a significant degree of anisotropy that affects the performance of the antenna, so a precise characterization and design must take into account account of this effect. The second is that the use of these materials may have a beneficial effect on the antennas, as in the case of Gurel and Yazgan, who have shown that the circular microstrip antenna with a correctly chosen uniaxial anisotropic substrate is more advantageous than the one with isotropic substrate exhibiting a wide bandwidth [4].

2. GREEN TENSOR TAKING ACCOUNT OF A PERMITTIVITY AND A PERMEABILITY OF TENSORIAL FORM

The method of moments is used to analyze our structure presented in Fig 1. The superconducting patch is placed on a dielectric which has a uniaxial anisotropy of electrical and magnetic type with the optical axis normal to the patch (see Fig 1) is characterized by a tensor permittivity and a tensor permeability on the form:

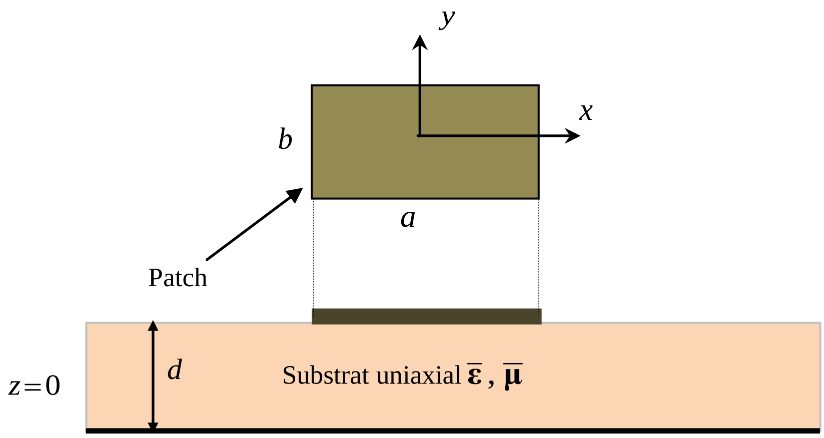

Fig. 1 Superconducting patch antenna made on a substrate with uniaxial anisotropy characterized by a tensorial permittivity and permeability.

$$\bar{\boldsymbol{\varepsilon}} = \varepsilon_0 \begin{bmatrix} \varepsilon_x & 0 & 0 \\ 0 & \varepsilon_x & 0 \\ 0 & 0 & \varepsilon_z \end{bmatrix} \tag{1}$$

$$\bar{\boldsymbol{\mu}} = \mu_0 \begin{bmatrix} \mu_x & 0 & 0 \\ 0 & \mu_x & 0 \\ 0 & 0 & \mu_z \end{bmatrix} \tag{2}$$

ε_0 and μ_0 are, respectively, the free-space permittivity and the free-space permeability. Equations (1) and (2) can be defined in the isotropic case by taking $\varepsilon_x = \varepsilon_z = \varepsilon_r$ and $\mu_x = \mu_z = \mu_r$.

Considering a temporal variation in $e^{i\omega t}$ and starting from the Maxwell equations in the Fourier domain, we can show that the transverse fields in the dielectric substrate $(0 \langle z \langle d)$ are written in terms of the longitudinal components $\tilde{E}_z$ and $\tilde{H}_z$

$$\tilde{E}_x(\mathbf{k}_s, z) = \frac{\mathrm{i}\,k_x}{k_s^2} \frac{\varepsilon_z}{\varepsilon_x} \frac{\partial \tilde{E}_z(\mathbf{k}_s, z)}{\partial z} + \frac{\omega\mu_0\mu_z\,k_y}{k_s^2} \tilde{H}_z(\mathbf{k}_s, z) \tag{3}$$

$$\tilde{E}_y(\mathbf{k}_s, z) = \frac{\mathrm{i}\,k_y}{k_s^2} \frac{\varepsilon_z}{\varepsilon_x} \frac{\partial \tilde{E}_z(\mathbf{k}_s, z)}{\partial z} - \frac{\omega\mu_0\mu_z\,k_x}{k_s^2} \tilde{H}_z(\mathbf{k}_s, z) \tag{4}$$

$$\tilde{H}_x(\mathbf{k}_s, z) = \frac{\mathrm{i}k_x}{k_s^2} \frac{\mu_z}{\mu_x} \frac{\partial \tilde{H}_z(\mathbf{k}_s, z)}{\partial z} - \frac{\omega\varepsilon_0\varepsilon_z\,k_y}{k_s^2} \tilde{E}_z(\mathbf{k}_s, z) \tag{5}$$

$$\tilde{H}_y(\mathbf{k}_s, z) = \frac{\mathrm{i}k_y}{k_s^2} \frac{\mu_z}{\mu_x} \frac{\partial \tilde{H}_z(\mathbf{k}_s, z)}{\partial z} + \frac{\omega\varepsilon_0\varepsilon_z\,k_x}{k_s^2} \tilde{E}_z(\mathbf{k}_s, z) \tag{6}$$

$\mathbf{k}_s = \hat{\mathbf{x}}k_x + \hat{\mathbf{y}}k_y$ is the transverse wave vector and $k_s = |\mathbf{k}_s|$ After carrying out some algebraic manipulations, we can put (3), (4), (5) and (6) in the form

$$\tilde{\mathbf{E}}(\mathbf{k}_s,z)=\begin{bmatrix}\tilde{E}_x(\mathbf{k}_s,z)\\ \tilde{E}_y(\mathbf{k}_s,z)\end{bmatrix}=\overline{\mathbf{F}}(\mathbf{k}_s)\cdot\begin{bmatrix}\dfrac{\mathrm{i}}{k_s}\dfrac{\varepsilon_z}{\varepsilon_x}\dfrac{\partial\tilde{E}_z(\mathbf{k}_s,z)}{\partial z}\\ \dfrac{\omega\mu_0\mu_z}{k_s}\tilde{H}_z(\mathbf{k}_s,z)\end{bmatrix}=\overline{\mathbf{F}}(\mathbf{k}_s)\cdot\begin{bmatrix}e^e(\mathbf{k}_s,z)\\ e^h(\mathbf{k}_s,z)\end{bmatrix} \tag{7}$$

$$\tilde{\mathbf{H}}(\mathbf{k}_s,z)=\begin{bmatrix}\tilde{H}_y(\mathbf{k}_s,z)\\ -\tilde{H}_x(\mathbf{k}_s,z)\end{bmatrix}=\overline{\mathbf{F}}(\mathbf{k}_s)\cdot\begin{bmatrix}\dfrac{\omega\varepsilon_0\varepsilon_z}{k_s}\tilde{E}_z(\mathbf{k}_s,z)\\ \dfrac{\mathrm{i}}{k_s}\dfrac{\mu_z}{\mu_x}\dfrac{\partial\tilde{H}_z(\mathbf{k}_s,z)}{\partial z}\end{bmatrix}=\overline{\mathbf{F}}(\mathbf{k}_s)\cdot\begin{bmatrix}h^e(\mathbf{k}_s,z)\\ h^h(\mathbf{k}_s,z)\end{bmatrix} \tag{8}$$

The exponents e and h denote the TM and TE waves, respectively, and

$$\overline{\mathbf{F}}(\mathbf{k}_s)=\frac{1}{k_s}\begin{bmatrix}k_x & k_y\\ k_y & -k_x\end{bmatrix}=\overline{\mathbf{F}}^{-1}(\mathbf{k}_s) \tag{9}$$

From equations (7), (8) and (9), we can show that

$$\mathbf{e}(\mathbf{k}_s,z)=\begin{bmatrix}e^e(\mathbf{k}_s,z)\\ e^h(\mathbf{k}_s,z)\end{bmatrix}=\overline{\mathbf{F}}(\mathbf{k}_s)\cdot\tilde{\mathbf{E}}(\mathbf{k}_s,z) \tag{10}$$

$$\mathbf{h}(\mathbf{k}_s,z)=\begin{bmatrix}h^e(\mathbf{k}_s,z)\\ h^h(\mathbf{k}_s,z)\end{bmatrix}=\overline{\mathbf{F}}(\mathbf{k}_s)\cdot\tilde{\mathbf{H}}(\mathbf{k}_s,z) \tag{11}$$

Expressions of $\tilde{E}_z$ and $\tilde{H}_z$ are

$$\tilde{E}_z(\mathbf{k}_s,z)=A^e\,\mathrm{e}^{-\mathrm{i}k_z^e z}+B^e\,\mathrm{e}^{\mathrm{i}k_z^e z} \tag{12}$$

$$\tilde{H}_z(\mathbf{k}_s,z)=A^h\,\mathrm{e}^{-\mathrm{i}k_z^h z}+B^h\,\mathrm{e}^{\mathrm{i}k_z^h z} \tag{13}$$

Where the spectral coefficients A^e, B^e, A^h and B^h are functions of the spectral variable k_s and

$$k_z^e=\sqrt{\frac{\varepsilon_x}{\varepsilon_z}}\sqrt{\left(\mu_x\varepsilon_z k_0^2-k_s^2\right)}\ ,\ k_z^h=\sqrt{\frac{\mu_x}{\mu_z}}\sqrt{\left(\mu_z\varepsilon_x k_0^2-k_s^2\right)}\ ,\ k_0^2=\omega^2\varepsilon_0\mu_0 \tag{14}$$

k_z^e et k_z^h are, respectively, the propagation constants of the waves TM and TE. After substitution of expressions of $\tilde{E}_z$ and $\tilde{H}_z$ given by (12) and (13) in (7) and (8), we obtain

$$\mathbf{e}(\mathbf{k}_s,z)=\mathrm{e}^{-\mathrm{i}\overline{\mathbf{k}}_z z}\cdot\mathbf{A}\ (\mathbf{k}_s)+\mathrm{e}^{\mathrm{i}\overline{\mathbf{k}}_z z}\,\mathbf{B}\ (\mathbf{k}_s) \tag{15}$$

$$\mathbf{h}(\mathbf{k}_s,z)=\overline{\mathbf{g}}\ (\mathbf{k}_s)\left[\mathrm{e}^{-\mathrm{i}\overline{\mathbf{k}}_z z}\,\mathbf{A}\ (\mathbf{k}_s)-\mathrm{e}^{\mathrm{i}\overline{\mathbf{k}}_z z}\,\mathbf{B}\ (\mathbf{k}_s)\right] \tag{16}$$

Where and are two vectors having components expressed as a function of the spectral coefficients A^e, A^h, B^e and B^h, and

$$\overline{\mathbf{k}}_z=\mathrm{diag}\left[k_z^e,k_z^h\right]\ ,\ \overline{\mathbf{g}}\ (\mathbf{k}_s)=\mathrm{diag}\left[\frac{\omega\varepsilon_0\varepsilon_x}{k_z^e},\frac{k_z^h}{\omega\mu_0\,\mu_x}\right] \tag{17}$$

By writing the equations (15) and (16) in the planes $z=0$ and $z=\mathrm{d}$ and by elimination of the unknowns $\mathbf{A}$ and $\mathbf{B}$, we obtain the matrix form

$$\begin{bmatrix}\mathbf{e}(\mathbf{k}_s,d^-)\\ \mathbf{h}(\mathbf{k}_s,d^-)\end{bmatrix}=\overline{\mathbf{T}}\begin{bmatrix}\mathbf{e}(\mathbf{k}_s,0^+)\\ \mathbf{h}(\mathbf{k}_s,0^+)\end{bmatrix} \tag{18}$$

with

$$\overline{\mathrm{T}} = \begin{bmatrix} \overline{\mathrm{T}}^{11} & \overline{\mathrm{T}}^{12} \\ \overline{\mathrm{T}}^{21} & \overline{\mathrm{T}}^{22} \end{bmatrix} = \begin{bmatrix} \cos(\overline{\mathrm{k}}_z d) & -\mathrm{i}\,\overline{\mathrm{g}}^{-1}\cdot\sin(\overline{\mathrm{k}}_z d) \\ -\mathrm{i}\,\overline{\mathrm{g}}\cdot\sin(\overline{\mathrm{k}}_z d) & \cos(\overline{\mathrm{k}}_z d) \end{bmatrix} \tag{19}$$

which combines **e** and **h** on both sides of the dielectric substrate. The continuity equations for the tangential components of the field are:

$$\tilde{\mathbf{E}}(\mathbf{k}_s, d^-) = \tilde{\mathbf{E}}(\mathbf{k}_s, d^+) = \tilde{\mathbf{E}}(\mathbf{k}_s, d) \tag{20}$$

$$\tilde{\mathbf{H}}(\mathbf{k}_s, d^-) - \tilde{\mathbf{H}}(\mathbf{k}_s, d^+) = \tilde{\mathbf{J}}(\mathbf{k}_s) = \begin{bmatrix} \tilde{J}_x(\mathbf{k}_s) \\ \tilde{J}_y(\mathbf{k}_s) \end{bmatrix} \tag{21}$$

By multiplying (20) and (21) by $\overline{\mathbf{F}}(\mathbf{k}_s)$ and using (10) and (11), we obtain

$$\mathbf{e}(\mathbf{k}_s, d^-) = \mathbf{e}(\mathbf{k}_s, d^+) = \mathbf{e}(\mathbf{k}_s, d) \tag{22}$$

$$\mathbf{h}(\mathbf{k}_s, d^-) - \mathbf{h}(\mathbf{k}_s, d^+) = \mathbf{j}(\mathbf{k}_s) \tag{23}$$

with $$\mathrm{j}(\mathrm{k}_s) = \begin{bmatrix} j^e(\mathrm{k}_s) \\ j^h(\mathrm{k}_s) \end{bmatrix} = \overline{\mathrm{F}}(\mathrm{k}_s)\,.\,\tilde{\mathrm{J}}(\mathrm{k}_s) \tag{24}$$

The transverse electric field must necessarily be zero on a perfect conductor, so for the perfectly conductive ground plane we have

$$\mathbf{e}(\mathbf{k}_s, 0^+) = \mathbf{e}(\mathbf{k}_s, 0^-) = \mathbf{e}(\mathbf{k}_s, 0) = \mathbf{0} \tag{25}$$

For the air region d^+ $(d \langle z \langle \infty, \varepsilon_x = \varepsilon_z = \varepsilon_r = 1 \ et\ \mu_x = \mu_z = \mu_r = 1)$ the expressions of e and h given by (15) and (16) become

$$\mathrm{e}(\mathrm{k}_s, d^+) = \mathrm{A}_0(\mathrm{k}_s)e^{-i k_z d^+} \tag{26}$$

$$\mathrm{h}(\mathrm{k}_s, d^+) = \overline{\mathrm{g}}_0(\mathrm{k}_s)\mathrm{A}_0(\mathrm{k}_s)e^{-i k_z d^+} \tag{27}$$

with $$k_z = (k_0^2 - k_s^2)^{1/2}, \quad \overline{\mathrm{g}}_0(\mathrm{k}_s) = diag\left[\frac{\omega\varepsilon_0}{k_z}, \frac{k_z}{\omega\mu_0}\right] \tag{28}$$

From (18), (22), (23), (25), (26), and (27) we obtain the following relation which links the current to the superconducting plate with tangential electric field on the corresponding interface:

$$\mathbf{e}(\mathbf{k}_s, d) = \overline{\mathbf{G}}(\mathbf{k}_s)\,.\mathbf{j}(\mathbf{k}_s) \tag{29}$$

Where $\overline{\mathbf{G}}(\mathbf{k}_s)$ is the dyadic spectral function of Green in the representation (TM, TE):

$$\overline{\mathrm{G}}(\mathrm{k}_s) = diag\left[G^{11}, G^{22}\right] = \left[\overline{\mathrm{T}}^{22}\,.\left(\overline{\mathrm{T}}^{12}\right)^{-1} - \overline{\mathrm{g}}_0\right]^{-1} \tag{30}$$

The spectral tensor of Green $\overline{\mathrm{Q}}(\mathrm{k}_s)$ connects the tangential electric field with the current in the plane of the patch is given by:

$$\tilde{\mathrm{E}} = \overline{\mathrm{Q}}.\tilde{\mathrm{J}} \tag{31}$$

with

$$\tilde{\mathrm{E}}(\mathrm{k}_s) = \begin{bmatrix} \tilde{\mathrm{E}}_x \\ \tilde{\mathrm{E}}_y \end{bmatrix}, \quad \tilde{\mathrm{J}}(\mathrm{k}_s) = \begin{bmatrix} \tilde{\mathrm{J}}_x \\ \tilde{\mathrm{J}}_y \end{bmatrix}, \quad \overline{\mathrm{Q}}(\mathrm{k}_s) = \begin{bmatrix} \mathrm{Q}_{xx} & \mathrm{Q}_{xy} \\ \mathrm{Q}_{yx} & \mathrm{Q}_{yy} \end{bmatrix}$$

The relationship between the diagonal tensor $\overline{\mathrm{G}}(\mathrm{k}_s)$ and the tensor $\overline{\mathrm{Q}}(\mathrm{k}_s)$ is as follows:

$$\overline{\mathrm{Q}}(\mathrm{k}_s) = \frac{1}{\mathrm{k}_s}\begin{bmatrix} \mathrm{k}_x & \mathrm{k}_y \\ \mathrm{k}_y & -\mathrm{k}_x \end{bmatrix} \cdot \overline{\mathrm{G}}(\mathrm{k}_s) \cdot \frac{1}{\mathrm{k}_s}\begin{bmatrix} \mathrm{k}_x & \mathrm{k}_y \\ \mathrm{k}_y & -\mathrm{k}_x \end{bmatrix} \tag{32}$$

In the structure studied, the patch is a superconducting plate, which has surface impedance Z_s at high frequency. In order to take Z_s into account, and in the field of Fourier vector transformations, the transverse electric field on the plane of the superconducting patchcan be written as a superposition of an electric field in the patch and another outside the patch, we have:

$$\mathbf{e}(\mathbf{k}_s, d) = \mathbf{e}^i(\mathbf{k}_s, d) + \mathbf{e}^o(\mathbf{k}_s, d) \tag{33}$$

Where $\mathbf{e}^i(\mathbf{k}_s, d)$ is the electric field in the patch (in), and $\mathbf{e}^o(\mathbf{k}_s, d)$ is the electric field outside patch (out). The electric field in the superconducting patch is given by:

$$\mathbf{e}^i(\mathbf{k}_s, d) = Z_s . \mathbf{j}(\mathbf{k}_s) \tag{34}$$

This surface impedance for the case of microwave, when the thickness of the patch e is less than three times the penetration length of LONDON, (by some approximations) is given by:

$$\mathrm{Z_s} = \frac{1}{\mathrm{e} \times \sigma} \text{ with } \sigma = \sigma_1 - i\sigma_2 \quad , \quad \sigma_1 = \sigma_n \left(\frac{T}{T_c} \right)^4$$

$$\sigma_2 = \frac{1}{\omega \mu_0 \lambda^2} \quad , \quad \lambda\ (T) = \frac{\lambda_0}{\sqrt{1 - \left(\frac{T}{T_c} \right)^4}}$$

Where T is the temperature, T_c is the transition temperature. By substituting equation (33) in equation (29) and taking into account equation (34):

$$\mathbf{e}^o(\mathbf{k}_s, d) = \left[\overline{G}(k_s) - Z_s \, \bar{I} \right] . \mathbf{j}(\mathbf{k}_s) \tag{35}$$

$\bar{I}$ denotes a unitary matrix of order 2. Using the Fourier inverse vector transform for equation (35), the transverse electric field outside (out) of the patch is as follows:

$$\mathbf{E}^o(\mathbf{r}_s, d) = \frac{1}{4\pi^2} \int_{-\infty}^{+\infty} \int_{-\infty}^{+\infty} \overline{\mathbf{F}}(\mathbf{k}_s, \mathbf{r}_s) . \left[\overline{G}(k_s) - Z_s \, \bar{I} \right] . \mathbf{j}(\mathbf{k}_s) dk_x dk_y \tag{36}$$

The application of the boundary condition, which requires the transverse electric field of equation (36) to vanish over the area of the superconducting patch, gives the following integral equation:

$$\int_{-\infty}^{+\infty} \int_{-\infty}^{+\infty} \overline{\mathbf{F}}(\mathbf{k}_s, \mathbf{r}_s) . \left[\overline{G}(k_s) - Z_s \, \bar{I} \right] . \mathbf{j}(\mathbf{k}_s) dk_x dk_y = 0, \quad (x, y) \in patch \tag{37}$$

Now, we can use the Galerkin method to solve the integral equation, and to obtain the resonance frequency, the bandwidth and the other parameters.

3. NUMERICAL RESULTS AND DISCUSSION

In order to validate the proposed approach, our results are compared with those of the open literature. We also compare our results with those reported recently in [5]. Particular care is devoted to studying the influence of the parameters of the uniaxial anisotropy on the bandwidth at temperatures far and near from the transition temperature Tc. knowing that bandwidth is extremely narrow when it comes to a high-temperature superconducting microstrip antenna relative to conventional antennas. Indeed, a small error on the determination of the frequency of resonance or in the design and the realization implies that the antenna can work outside its bandwidth, and which will have a direct influence on the characteristics of the antenna. For this reason, we have worked on the possibilities that can help to improve the bandwidth for a Tc high-temperature superconducting microstrip antenna, without affecting the advantages of this antenna over the conventional antenna, namely: high gain, the low weight aspect, ...

3.1 Comparison of results with literature

In order to validate our program, the results found in Table 1 are compared with the results obtained from the magnetic sidewall cavity model of Richard et al [6].

Table -1 comparison of our results with those obtained via the cavity model combined with electromagnetic knowledge for various anisotropic and non-magnetic materials: *a*x*b*=2025μm x 1350μm, *d*=14.85μm, σn=10^6 S/m, λ0 =140 nm, Tc=89 K, e=350 nm, et T=50 K

Diélectrique	**(εx, εz)**	**our results fr (GHZ)**	**cavity model [6]GHZ**	**Erreur %**
Saphir	(9.4, 11.6)	32.290	32.282	0.025
Epsilam-10	(13, 10.3)	34.268	34.254	0.041
Nitrure de bore	(5.12, 3.4)	59.509	59.609	0.16
PTFE	(2.88, 2.43)	70.265	70.527	0.37

All these results have been obtained for a patch antenna with a YBCO superconducting thin film, with: *a*x*b*=2025µm x 1350µm, *d*=14.85µm, σn=10^6 S/m, λ0 =140 nm, Tc=89 K, e=350 nm, et T=50 K ; this patch is stamped on an anisotropic substrate. It should be noted that the operating temperature is equal to T = 50 K, and the anisotropic and non-magnetic materials used on the cavity model with magnetic sidewalls [6] are Sapphire, Epsilam-10, boron nitride, and PTFE. It is very clear that our results are very close to those obtained via the magnetic side wall cavity model [6] and the error is very small and it is far from 1%.

With these results we can validate our program in order to use it on other anisotropic materials (electrical type and magnetic type) and see the influence of the various parameters of superconducting antennas with high critical temperature and with anisotropic substrate on their performances, to know: bandwidth, resonant frequency, and others.

3.2 Effect of uniaxial electric anisotropy

3.2.1 Variation of εx

In this part, we will see the effect of the anisotropy ratio AR1 = εx / εz on the resonance frequency and the bandwidth. The value of the relative permittivity was fixed along the optical axis εz and the value of the relative permittivity along the two axes perpendicular to the optical axis εx was changed in order to have the values of AR1 between 0.5 and 2. The patch (axb = 2550 x 1700 µm size) is manufactured with a superconducting YBCO ($YBa_2Cu_3O_7$) thin film having as parameters µr=1, εz=2.32, $\sigma_n = 10^6$ *S /m*, $\lambda_0 = 140\,nm$, *Tc*=89K, and *e*=350*nm*; the operating temperature is T = 50K. Calculations are also made for a thin substrate of 153 µm.

Note for Table 2 (εx varies, and εz fixed) that for an increase of AR1 (following an increase of εx) from 0.5 to 2, the frequency decreases from 54.502 GHZ to 52.524GHZ, ie a fractional decrease of 3.63%. The same remark can be made for the bandwidth, the fractional decrease is 4.52%. The same percentages of variation and influence on frequency and bandwidth are observed for temperatures near from Tc (see Table 3).

Table -2 Effect of uniaxial anisotropy of electrical type (variation of εx): axb=2550µm x 1700µm ,*d*=153 µm, σn=10 S/m, λ0 =140 nm, Tc=89 K ,e=350 nm, T=50 K , εz= 2.32, µx = 1, µz= 1

εx	**AR1=εx/ εz**	**Resonance frequency (GHZ)**	**Bandwidth %**
1.16	0.5	54.489	5.300
1.74	0.75	54.090	5.246
2.32	1	53.729	5.202
2.9	1.25	53.396	5.164
3.48	1.5	53.085	5.128
4.06	1.75	52.791	5.094
4.64	2	52.512	5.060

Table -3 Effect of variation of εx (AR1) on the frequency (fr) and the bandwidth (BW) for temperatures near from Tc

***d*=153 µm**		**T=88K**		**T=88.5K**		**T=88.8K**		**T=88.9K**	
εx	**AR1=εx/ εz**	**fr(GHZ)**	**Bw%**	**fr(GHZ)**	**Bw%**	**fr(GHZ)**	**Bw%**	**fr(GHZ)**	**Bw%**
1.16	0.5	54.257	5.361	54.048	5.706	53.756	7.295	53.812	8.893
4.64	2	52.287	5.117	52.085	5.448	51.790	7.027	51.833	8.699

3.2.2 Variation of εz

Considering now the results summarized in Table 4:

If we takes the same values of AR1 (from 0.5 to 2), but we changes the values of εz and fixes εx to have the negative anisotropy (εx>εz) or positive (εx <εz). For the same other parameters of the antenna, we obtain an increase of the frequency from 28.415GHZ to 52.512GHZ, a fractional change of 84.73%, and for the bandwidth it change from 1.233 to 5.060, a fractional change of 309.38 %. The influence of εz on the frequency and the bandwidth is greater than that of εx, and more than it is weak more than it increases the two parameters (frequency and bandwidth).

For a larger substrate value (d = 306µm), the results are shown in Table 6, which indicates that there is an increase in frequency from 27.561GHZ to 47.880GHZ, a fractional change in 73.72%, and for the bandwidth it change from 2.685 to 9.907, a fractional change of 268.97%. But we also note that for each value of AR1, the value of the frequency in the thin case is greater than its value in the thick case. So to provide an additional increase in bandwidth, the thickness of the substrate can help to do by increasing the thickness, but just to acceptable values so as not to lose the low-weight aspect highly desirable in practice, and for avoid excitation of surface waves that strongly affect the performance of the antenna.

In Table 5, we note that for temperatures very close to Tc, the effect of variation of εz on the value of fr is almost the same as for temperatures far from Tc (T = 50K), but for effect on the bandwidth it is different, because as we approach Tc, the percentage of influence of εz on the bandwidth decreases (from 309.38% for T = 50K to 60.61% for T= 88.9 K).

Table -4 Effect of uniaxial anisotropy of electrical type (variation of εz):axb=2550µm x 1700µm, ***d*=153 µm**, σn=10 S/m, λ0 =140 nm, Tc=89 K, e=350 nm, T=50 K , εx= 4.64, µx = 1, µz= 1

εx	**AR1= εx/ εz**	**εz**	**fr(GHZ)**	**Bw %**
4.64	0.5	9.28	28.426	1.236
4.64	0.75	6.18	34.228	2.002
4.64	1	4.64	38.916	2.741
4.64	1.25	3.71	42.942	3.417
4.64	1.5	3.09	46.487	4.039
4.64	1.75	2.65	49.646	4.583
4.64	2	2.32	52.512	5.060

Table -5 Effect of variation of εz (AR1) on fr and Bw for temperatures near from Tc

***d*=153 µm, εx=4.64**		**T=88K**		**T=88.5K**		**T=88.8K**		**T=88.9K**	
εz	**AR1**	**fr(GHZ)**	**Bw %**	**fr(GHZ)**	**Bw %**	**fr(GHZ)**	**Bw %**	**fr(GHZ)**	**Bw %**
9.28	0.5	28.306	1.292	28.190	1.505	27.923	2.802	27.760	5.416
2.32	2	52.287	5.117	52.085	5.448	51.790	7.027	51.833	8.699
influence percentage of εz on fr and Bw in%		84.73%	296.05%	84.76%	261.99%	85.47%	150%	86.71%	60.61%

Table -6 Effect of uniaxial anisotropy of electrical type (variation of εz):axb=2550µm x 1700µm, ***d*=306 µm**, σn=10 S/m, λ0 =140 nm, Tc=89 K, e=350 nm, T=50 K , εx= 4.64, µx = 1, µz= 1

εx	**AR1= εx/ εz**	**εz**	**fr(GHZ)**	**Bw %**
4.64	0.5	9.28	27.561	2.685
4.64	0.75	6.18	32.696	4.282
4.64	1	4.64	36.731	5.737
4.64	1.25	3.71	40.121	7.041
4.64	1.5	3.09	43.046	8.166
4.64	1.75	2.65	45.603	9.112
4.64	2	2.32	47.880	9.907

4. CONCLUSION

In this work, results concerning the resonant frequency and the bandwidth of a rectangular microband antenna with superconducting patch were presented. We validated the method by comparing our results with those of the literature for four anisotropic and non-magnetic materials. These anisotropic materials are Sapphire, Epsilam-10, Boron Nitride and PTFE. A good agreement was obtained between our results and those calculated by the cavity model with magnetic sidewalls. The effect of electrical anisotropy and the influence of εx and εz on frequency and bandwidth have also been studied. Contrary to what was mentioned in [5], we found that the parameters of electrical anisotropy (AR1) cannot alone determine the increase or decrease of the bandwidth, but we must take into account the two values of the permittivity; namely εx and εz. The effect of these parameters, already mentioned, on the frequency and the bandwidth, is recalculated for the temperatures far from Tc and near from Tc, where it has been found that the temperature can help to improve the bandwidth with interesting values.

REFERENCES

[1]. N. Sekiya, A. Kubota, A. Kondo, S. Hirano, A. Saito, S. Ohshima, ‘‘Broadband superconducting microstrip patch antenna using additional gap-coupled resonators.’’ Physica C 445–448 (2006) 994–997.

[2]. O. Barkat, A. Benghalia, ‘‘Radiation and resonant frequency of superconducting annular ring microstrip antenna on, uniaxial anisotropic media.’’ J. Infrared MilliTerahz Waves 30 (2009) 1053–1066.

[3]. Y. Tighilt, F. Bouttout, A. Khellaf, ‘‘Modelling and design of printed antennas using neural networks.’’ Int. J. RF Microwave CAE 21 (2011) 228–233.

[4]. Ç.S. Gürel, E. Yazgan, ‘‘Characteristics of a circular patch microstrip antenna on uniaxially anisotropic substrate.’’ IEEE Trans. Antennas Propag.52 (2004) 2532– 2537.

[5]. S. Benkouda, A. Messai, M. Amir, S. Bedra, T. Fortaki ‘‘Characteristics of a high Tc superconducting rectangular microstrip patch on uniaxially anisotropic substrate.’’ Physica C 502 (2014) 70–75.

[6]. M.A. Richard, K.B. Bhasin, P.C. Claspy, ‘‘Superconducting microstrip antennas: an experimental comparison of two feeding methods.’’ IEEE Trans. Antennas Propag. 41 (1993) 967–974.